

# Animating Stock Markets\*

Tomasz Kaczmarek<sup>†</sup>

Kuntara Pukthuanthong<sup>‡</sup>

September 11, 2024

## Abstract

Our study introduces Variational Recurrent Neural Networks (VRNNs) for stock price prediction through a cinematic approach: transforming complex market data into dynamic, graph-based narratives that unfold like a movie. Analyzing S&P 500 constituents from 1993 to 2021, we achieve Sharpe ratios of 2.94 for equally weighted and 2.47 for value-weighted portfolios. After adjusting for a transaction cost, our model's Sharpe ratio remains twice as high as that reported by Jiang et al. (2023). Our method achieves an alpha of 55 weekly basis points, adjusted for established risk factors. Our model's prediction of pixel changes robustly forecasts weekly returns, accounting for various price trend strategies and firm characteristics. The correlation of our predicted returns with institutional trading is substantial and, to a lesser extent, with retail trading.

**Keywords:** Variational Recurrent Neural Networks, Graphs, Predictability, S&P500

**JEL Codes:** G00, G11, G12

---

\*The full version of the paper can be read at

[https://www.kuntara.net/uploads/1/1/4/9/114945401/animating\\_stock\\_marketets\\_old - 9.pdf](https://www.kuntara.net/uploads/1/1/4/9/114945401/animating_stock_marketets_old - 9.pdf).

This work was partly supported by the National Science Foundation under Grant No. OAC-1919789. We thank Leland Bybee (discussant), Charles Clark, Andrew Patton, Seth Pruitt, Guofu Zhou, and seminar participants at the Midwest Finance Association meeting in Chicago in 2024, and the Finance Future Info in Stockholm, Sweden, May 2024.

<sup>†</sup>Tomasz is from the Department of Investment and Financial Markets, Institute of Finance, Poznan University of Economics and Business, Poland. Email: tomasz.kaczmarek.sci@gmail.com. Polish National Agency partly funded Tomasz's research for Academic Exchange within the Bekker Programme, grant number BPN/BEK/2021/1/00404/U/DRAFT/00001, and National Science Centre, Poland, grant number 2021/41/N/HS4/02344. For Open Access, the author has applied a CC-BY public copyright license to any Author Accepted Manuscript (AAM) version arising from this submission.

<sup>‡</sup>Kuntara is from Trulaske College of Business at the University of Missouri, Columbia, MO, USA. Email: pukthuanthongk@missouri.edu

# 1 Introduction

The endeavor to accurately predict future stock price movements has long been at the heart of financial economics. This pursuit, fundamental to trading strategies and risk management, is complex due to the multifaceted nature of financial markets. Traditional models, which predominantly rely on numerical time-series data, often grapple with the market's evolving patterns, pronounced volatility, and susceptibility to various external influences. Such challenges underscore the pressing need for a more innovative and adaptable approach to forecasting.

Financial markets are not static entities; they pulsate with life, evolve, and react to many stimuli. This dynamism is reminiscent of frames in a cinematic reel, where each frame, though a standalone snapshot, is intrinsically linked to its predecessor, painting a broader narrative. Similarly, today's stock market reflects yesterday's, and one must grasp this sequential relationship to forecast tomorrow's. It is here that our research introduces a paradigm shift. By harnessing the power of Variational Recurrent Neural Networks (VRNNs), we aim to predict stock price trends, translating daily price changes into graphical representations and training the model to forecast future trajectories.

To elucidate the significance of this approach, consider the dot-com bubble of the late 1990s and early 2000s. A static snapshot during the bubble's zenith would portray tech stocks as the golden geese of the era. However, a more 'animated perspective reveals a sequence: the mid-1990s rise of the internet, the late 1990s' exponential growth in tech valuations, the bubble's peak around 2000, and its eventual burst in the early 2000s. This sequence, akin to movie frames, provides a holistic understanding of the bubble's buildup, climax, and denouement.

The Variational Recurrent Neural Network (VRNN) model exhibits a distinctive capability to integrate and leverage historical events, such as mergers and acquisitions, into its predictive analysis, which sets it apart from conventional time-series forecasting methods. Unlike traditional models that might analyze data in isolation or within a static framework,

the VRNN dynamically incorporates a sequence of data points, effectively 'remembering' significant market events and their aftermath within its predictions. This is achieved through the VRNN's sophisticated architecture, which melds the sequential memory strengths of Recurrent Neural Networks with the deep learning prowess of Convolutional Neural Networks and the probabilistic approach of Variational Autoencoders. As a result, VRNN can offer nuanced insights into future market behavior by understanding the long-term implications of pivotal events far beyond the immediate impact period. This quality makes the VRNN particularly adept at navigating the complexities of financial markets, where the ripples of major events can influence market dynamics well beyond their occurrence, providing a more informed and holistic approach to predicting stock movements compared to other methodologies.

In finance, researchers have been using machine learning to predict asset returns and measure risk premiums. Such studies include those conducted by Feng, He, and Polson (2018), Chen, Pelger, and Zhu (2023), and Gu, Kelly, and Xiu (2020). However, many of these studies have relied on traditional feed-forward neural networks that only consider features of fixed dimensions and do not consider the longer-term sequential dependency of asset prices and returns. There is a limitation because asset returns are known to follow both short-term and long-term patterns, such as return momentum and reversal patterns. To address this issue, it is important to model the sequential dependence of asset returns when designing strategies that rely on such data. Our study contributes to this literature by exploring the mechanisms and performance of various deep sequence modeling techniques, specifically in estimating the risk premiums of U.S. equities. The same analogy applies to weather forecasts, using frames instead of single graphs (Bi et al., 2023).

In this way, frames form a recurrence (or sequence) in the model that is also a characteristic part of financial markets. That is why predicting financial markets with their dynamics as frames is better than comparing two static graphs (for example, a graph with observed and predicted prices).

Our research shifts the focus from the commonly preferred return predictions to the direct forecasting of asset prices. This approach is grounded in the practical utility of knowing future price levels for trading decisions. Price forecasts provide specific, actionable information, such as precise future price levels, directly applicable to trading strategies like setting stop-loss orders or planning entry and exit points. Return predictions do not offer this specificity directly, which requires additional steps to translate returns into actionable price levels.

The autocorrelation in price data is a key advantage our model leverages. Prices tend to follow a pattern where current levels are closely related to past levels, making them more predictable. This starkly contrasts returns, which generally show less autocorrelation, making them more challenging to predict accurately. Although it is true that the financial community often focuses on returns due to their normalized nature and ease of comparison across different assets, our research suggests that the direct prediction of prices can offer more immediate and actionable insights for traders and investors.

Our study focuses on predicting the prices of the S&P500 constituents to calculate our Sharpe ratio (SR) from weekly returns from 1993-2021. We find that equally weighted portfolios had an SR of 2.94, while value-weighted portfolios had an SR of 2.47.

In comparison, Jiang, Kelly, and Xiu (2023) report a lower equal-weighted SR of 0.78 and a value-weighted SR of 0.96. Although our SR is surprisingly high, our turnover is also high, at 1121% and 1156% for equal-weighted and value-weighted portfolios, respectively. This is compared to the turnover of 676% and 693% from Jiang et al (2023). Therefore, we factor in transaction costs of 10 basis points, resulting in an SR of 1.61 and 1.21 for equal-weighted and value-weighted portfolios, respectively.<sup>1</sup>

Our analysis reveals that increased predicted pixel changes are inversely associated with 1-month momentum, return volatility, and the bid-ask spread. After adjusting for moving average momentum and various firm characteristics, we observe that predicted pixel changes

---

<sup>1</sup>This adjustment is in line with the standard trading cost for stocks exceeding the 80th size percentile of the NYSE (Frazzini, Israel, & Moskowitz, 2018; Ke, Kelly, & Xiu, 2019).

strongly increase weekly returns, confirming VRNN’s strong performance. Additionally, we show that financial institutions are actively engaging with our strategy. Intriguingly, our findings indicate that retail traders are implementing our strategy, albeit significantly less than institutional traders.

Our trading strategy involves longing stocks in the highest quintile of predicted change in pixel and selling the opposite while controlling for prominent factors from seminal models, such as the six-factor model of Fama and French (2018), the five-factor model of Hou, Mo, Xue, and Zhang (2021), the behavioral model of Daniel, Hirshleifer, and Sun (2020), short-term reversal, and long-term reversal factors. Our alpha from this strategy is approximately 55 basis points per week. In other words, we buy stocks expected to increase the most in price and sell stocks expected to decrease the most in price based on the model’s predictions from the visual representation of their price movements.

It is important to note that our strategy is based on the constituents of S&P500 stocks, which are large-cap, highly liquid and have low transaction costs. Predicting outcomes in this market is notoriously difficult, which makes our average SR of over 1.4 after transaction costs still quite high.

Our study introduces a new approach to predicting future US stock prices as video sequences using Variational Recurrent Neural Networks (VRNNs). This methodology exploits the synergistic strengths of Recurrent Neural Networks (RNNs), Variational Autoencoders (VAEs), and Convolutional Neural Networks (CNNs) to capture both temporal and spatial relationships between price movements.

To understand our model, it is helpful to compare it with the process of creating a movie. Recurrent Neural Networks (RNNs) act like scriptwriters, capturing the storyline of stock prices over time. They remember what happened in previous frames (or days) to make educated guesses about what comes next. Variational Autoencoders (VAEs) are like the special effects team, adding depth and dimension to our movie. They help our model understand the range of possible future scenarios by learning to represent complex data in

simpler forms. Lastly, Convolutional Neural Networks (CNNs) work as cinematographers, focusing on the visual patterns within each frame. They identify important features in the data, such as sudden price spikes or drops, much as a camera focuses on key elements in a scene. Together, these technologies enable our model to generate dynamic and predictive video sequences of stock prices, capturing the flow of time and the intricate patterns within the data.

Complexity in financial market dynamics often cannot be adequately captured through simple numerical forecasts. The ability of our methodology to predict more than mere price movements - such as volatility trends and trading volumes - presents a much more holistic view of the market's future. This depth of insight is invaluable in strategic decision-making processes, helping investors better manage risk and potential returns.

Our results demonstrate the capacity of the VRNN model to accurately forecast the trajectory of market data changes for the next ten trading days. These forecasts cover closing prices, maximum and minimum prices, the direction of a 20-day moving average, and volumes. This multidimensional output offers an enriched prediction of market trends and equips investors with a holistic understanding of the anticipated market performance, empowering them to effectively strategize their investment decisions.

Understanding stock price reactions to company announcements is paramount in the complex world of financial markets. To deepen our understanding of our approach, we compare ours with traditional prediction models that employ an expanded window approach, such as momentum and short-term and long-term reversals. We meticulously consider all past stock reactions to predict future movements. For instance, when predicting a stock's reaction on the 30th day, these models would analyze the stock's behavior from the 1st day to the 29th day. While comprehensive, this method treats each day's reaction as an isolated event, potentially overlooking the evolving nature of stock reactions.

Consider a scenario with Microsoft, a tech giant known for its diverse product portfolio and strategic acquisitions. Over several months, Microsoft has released updates to its

Windows operating system, launched new Surface devices, and announced collaborations with various tech companies. On a particular day, Microsoft announces a groundbreaking acquisition of Activision Blizzard, a leading video game publisher. Traditional models, which analyze all past stock reactions, might struggle to predict the market's response to this unexpected event accurately. Without a similar prior acquisition announcement as a reference, these models might base their prediction on the average of all past reactions to Microsoft's announcements, potentially underestimating the impact of this significant acquisition.

In contrast, a VRNN approach would consider the dynamic 'memory' of Microsoft's stock reactions to various events over time. This memory captures evolving patterns, such as how the stock has historically responded to different announcements, including product launches, updates, and acquisitions. When Microsoft announces the acquisition of Activision Blizzard, the VRNN, informed by its memory of past reactions, would analyze this new event in the context of Microsoft's historical patterns. It might recognize the acquisition announcement as a significant positive development, similar to past positive announcements, and predict a strong market reaction based on the cumulative knowledge of how the stock has reacted to similar events in the past.

Consider a technology company that is active in announcing new products, updates, and various business developments over several months. On the 32nd day, they announce a significant merger with another tech giant. Traditional predictive models, which analyze a broad range of past events, might not perform well in this scenario. These models typically average the stock's reactions to past announcements. Still, if they have not encountered a merger announcement before, their prediction for the stock's reaction to the merger might be off, simply averaging out the responses to less significant news.

This is where the Variational Recurrent Neural Network (VRNN) approach shines. The VRNN has a dynamic 'memory' that tracks and learns from the stock's reactions, adapting to new information. It recognizes patterns in how the stock price responds to different announcements. For example, if the stock has shown increasingly positive reactions to part-

nership announcements over time, the VRNN uses this information to understand the context better. When the merger announcement comes—a type of super partnership—the VRNN, drawing on its nuanced memory of past reactions, can predict a stronger-than-average response to this news. Unlike traditional models, the VRNN does not just look at past reactions in isolation; it understands the evolving context and significance of different types of announcements, allowing it to make a more informed prediction about the stock’s reaction to the merger.

As another example, consider a tech stock that, over 10 days, reacts to a series of product announcements with the following percentage changes: [1%, 2%, -1%, 0.5%, 1.5%, 2%, -1.5%, 0.5%, 1.5%, 2.5%]. A discernible pattern emerges: modest gains often precede a slight dip. Using a traditional expanded window approach, the model would analyze all previous percentage changes to predict the stock’s reaction on the 11th day, treating each as an independent data point. The prediction might be a simple average, suggesting a modest gain.

However, a VRNN approach, with its dynamic memory, would recognize the sequence’s rhythm. It would ‘remember’ the stock’s tendency to dip after a series of gains. Given that the last three days before the 11th showed gains, the VRNN might predict a dip for the 11th day, aligning more closely with the stock’s observed behavior. This illustrative example underscores the VRNN’s potential to capture intricate temporal patterns in stock price reactions, offering a nuanced lens for financial forecasting.

In this research, we delve into VRNN’s potential to capture the sequential and evolving nature of stock price reactions, offering a fresh perspective in the ever-complex realm of financial forecasting.

The VRNN model uniquely combines the strengths of Recurrent Neural Networks (RNNs), Variational Autoencoders (VAEs), and Convolutional Neural Networks (CNNs) to process and predict complex financial data like stock prices with superior accuracy. The RNN component is crucial for handling sequential data, utilizing a hidden state as a form of memory



to capture and leverage information from previous time steps. This allows the VRNN to maintain continuity and recognize temporal patterns in stock price movements.

The VAE element introduces a probabilistic layer to the model, enabling it to handle the inherent uncertainty and variability in financial markets. By encoding data into a probabilistic space, the VAE allows the VRNN to make informed predictions despite ambiguous or incomplete information, assessing the likelihood of various outcomes based on past patterns.

Complementing the RNN and VAE, the CNN component excels in processing spatial data and identifying complex patterns. In financial forecasting, CNN can analyze the spatial relationships in market data—such as the arrangement of price movements within a given timeframe—to detect patterns that might not be immediately apparent from a purely temporal analysis.

When these three components work together, the VRNN leverages the CNN’s ability to dissect spatial patterns, the RNN’s capacity to understand and remember sequences, and the VAE’s proficiency in managing uncertainty. This integrated approach allows the VRNN to capture a more comprehensive picture of market dynamics, making it adept at predicting stock prices with depth and accuracy that surpasses models relying solely on the CNNs or any single component.

The synergy between the RNC’s sequential memory, the VAE’s probabilistic insights, and the CNN’s spatial pattern recognition equip the VRNN with a multifaceted understanding of financial data. This enables the model to anticipate price movements more effectively by considering the order of events and the complex interplay of factors influencing market behavior. As a result, the VRNN stands out for its ability to deliver nuanced and robust price predictions, harnessing the combined power of RNN, VAE, and CNN technologies to navigate the complexities of financial forecasting.

## 2 Contribution and Related Research

Our study contributes to financial economics in multiple ways. Not only does it introduce a novel VRNN-based methodology for predicting future stock prices, but it also paves the way for the application of advanced machine learning techniques in financial forecasting. The multidimensional output of our model aids in making informed investment decisions by offering a rich and nuanced understanding of market trends.

Numerous studies have explored the influence of images, graphs, and colors on investment decisions and stock prices. However, examining graphs and machine learning and their impact on stock prices is still in its early stages. The first paper to utilize machine learning on images was conducted by Obaid and Pukthuanthong (2022). They use CNN to convert images into a sentiment score and demonstrate that photo sentiment is more predictive than text sentiment.

Jiang et al. (2023) is the first paper that uses graphs to predict returns; naturally, their concept is closest to ours, though they are not the same. To illustrate, they transform historical price and trading data into two-dimensional images and use CNN to analyze graphs and predict prices based on patterns. We differ in several aspects from their approach.

First, our approach leverages VRNNs to predict stock market price movements. We use visual representations in video frames, utilizing image-based machine learning models. Our VRNN models combine the strengths of RNNs, VAEs, and CNNs to handle complex sequential data efficiently. RNNs capture the temporal dependencies in stock prices, remembering past price movements to predict future trends. VAEs compress and encode the data, handling uncertainty in price movements. CNNs extract spatial features from each frame, identifying patterns in price movements. Unlike CNNs, which only use static individual 2D images, our VRNN models predict price movements as sequential frames akin to a ‘video.’ This approach enables our models to capture the sequential dependencies inherent in financial time series data, providing a more dynamic and comprehensive understanding of stock price movements

Second, our predictions focus on the constituents of the S&P 500 index, emphasizing short-term forecasts and stocks with high liquidity. In contrast, Jiang et al. (2023) analyzes data from all companies listed on the NYSE, AMEX, and NASDAQ. While we do not specify a particular frequency for portfolio rebalancing, Jiang et al. (2023) find that their highest Sharpe ratio is obtained with a five-day rebalancing period. On the other hand, their Sharpe ratios for more extended rebalancing periods of 20 days and 60 days were significantly lower.

Our methodology is ideal for investors who frequently rebalance their portfolios and engage actively with their investments. This approach suits those in trading roles that require higher turnover or investors seeking more active involvement. The methodology employed by Jiang et al., 2023 is more suitable for investors interested in medium to long-term strategies as they analyze static 2D images representing longer-term trends. However, this approach may not provide insights for short-term, quick decision-making.

Third, regarding liquidity, we focus on S&P 500 index companies, ensuring high liquidity and lower transaction costs. This is particularly advantageous for institutional investors who need to make significant transactions without impacting the market price significantly. On the other hand, their study covers all companies listed on the NYSE, AMEX, and NASDAQ, providing broader market coverage and potentially diversifying investment options. However, this comes from lower liquidity and potentially higher transaction costs from tiny stocks.

Fourth, our model forecasts accuracy by predicting the direction and scale of price changes, closing prices, maximum and minimum prices, the direction of a 20-day moving average, and volumes. This level of detail provides investors with a comprehensive understanding of future stock performance. The video frames generated by our model depict stock price movements over time, creating a dynamic and informative time-series-like visual output. Our approach allows practitioners to consider short-term and medium-term investment strategies based on predicted movements for the next ten trading days.

In comparison, Jiang et al. (2023) predict the probability of returns going up and down, which provides a binary perspective on price movements. While this approach is more

straightforward and may be easier for practitioners to interpret, it lacks the detailed information and accuracy of our dynamic, time-inclusive VRNN approach. Our methodology is particularly advantageous for investors engaged in high-frequency trading strategies, as it offers a more nuanced understanding of price movements. By predicting the direction and magnitude of price changes, our approach enables traders to make more informed decisions, optimizing their trading strategies for better performance in a fast-paced market environment.

While both studies use graphical representations in their methodology, the critical difference lies in the type of financial variable being predicted (returns vs. prices) and how images are used in the prediction. Jiang et al. (2023) use their predicted probabilities to sort portfolios to create portfolios that are likely to perform well based on the predicted direction of stock prices. In contrast, we generate future images of price trends and then decode these images to predict future prices.

It is worth noting that, like all predictive algorithms, our model has certain limitations. However, despite these limitations, it offers a detailed and multi-dimensional view of future market dynamics. The interpretation of the output may be more complex than more straightforward binary predictions, but our approach is highly effective. While some other methods, such as the methodology of Jiang et al. (2023), which utilizes static 2D images, may be less computationally intensive, our results are focused on large and highly liquid stocks. We are working on all stocks in the same sample as (2023) to disentangle which step contributes to our performance. The result will be publicly available soon. The high predictability threshold of these large stocks suggests that our model may also perform well with smaller stocks.

Despite these constraints, we firmly believe that our work heralds a significant step forward in financial forecasting. It underscores the potential of innovative machine learning methodologies in generating nuanced, visually intuitive, and comprehensive market forecasts, thus adding a robust tool to the arsenal of investors and financial analysts. Our study is a

foundation for future research in this exciting and promising arena of graph-based financial predictions.

### **3 Animated Market Data**

The advent of machine learning in finance has opened a gateway for sophisticated and efficient forecasting methods. However, the complexity of financial markets and the multiplicity of factors affecting them raise significant challenges for these methods. Here, we present a novel approach to address this complexity by leveraging animated market data. While stock price changes are typically viewed statically, they exhibit a dynamic nature, akin to frames in a movie, where each frame is closely related to its predecessor. In the same vein, current stock market figures reflect their past performances. Thus, forecasting future price movements hinges significantly on understanding this sequential relationship, which can be effectively captured through animation.

#### **3.1 Multivariate Graphical Data Input**

The incredible information capacity of visuals serves as the bedrock of our research. Single graphs can convey a multitude of information simultaneously, making interpretation more accessible. Firstly, a single chart can depict an entire data series related to a specific variable, such as a stock's historical prices over a specified period. Secondly, one chart can encapsulate multiple time-series data simultaneously, like overlaying stock prices, moving averages, and trading volumes. Thirdly, in addition to portraying price data on the day of observation, graphs can present information about their variability, broadening the data spectrum while maintaining clarity. Lastly, the ability to use different colors in graphics makes it easier to discern differences between observation points for each series.

In our study, we harness the power of visuals to capture past closing prices, maximum and minimum prices, 20-day moving averages, and trading volume. We independently generate

each image for full control over its content and the optimal arrangement of all elements in the chart. Jiang et al. (2023) inspire our chart construction. To our knowledge, we are the first study to generate future graphs.<sup>2</sup> Instead of processing the image to predict the return direction, we incorporate several modifications to enhance the image clarity for machine learning algorithms that will process them later. Figure 1 visualizes the comparison between graphs from this study and those used by Jiang et al. (2023). The left graph we propose displays 20 days of historical daily observations and predicts the market data for up to 10 days in the future. Meanwhile, the graph on the right, constructed by Jiang et al. (2023), also uses 20 historical daily observations but predicts the direction of the price for 5, 20, or 60 days. It is important to note that their output is the probability of return direction, while our predictions are prices up to 10 days ahead.

Primarily, closing prices are the most critical elements in charts, whether the predictive task is forecasting returns, price changes, or prices themselves. Hence, we increase the visibility of prices in the chart by modifying the typical OHLC (Open, High, Low, Close) chart, where the closing price is merely a small dot, to a line chart connecting closing prices. This line running through the entire chart is easily perceptible to the human eye and machine learning algorithms.

Secondly, we omit to present opening prices, which do not provide significant predictive value and are challenging to overlay when drawing closing prices as a line. Thirdly, we color-code each of the utilized series. The closing prices are white, the trading volume is light grey, the high-low (HL) bars are darker grey, and the moving average is the darkest grey against a black background. This color differentiation makes it easier to distinguish, for example, between closing prices and the moving average. Importantly, closing prices are always overlaid last, so they remain visible irrespective of other data. The following section discusses further modifications in chart creation that tailor our images to the main objective of our study - capturing market dynamics through image animation.

---

<sup>2</sup>Jiang et al. (2023) predict the probability of stocks going up and down.

## 3.2 Market Dynamics as Video Frames

Stock price changes on day  $t$  are conditional on the market information from the  $n$  preceding days, much like the content of the last video frame depends on the information in the previous frames. Figure 2 illustrates the analogy between consecutive video frames in the popular testing database ‘Bair Push Dataset’ (Ebert, Finn, Lee, & Levine, 2017) used to evaluate the predictive abilities of machine learning models dedicated to forecasting subsequent video frames and video frames generated by us to predict future stock prices. The changes in the content of each frame are minor, as most of the information repeats in each of them. The difference between the frames induces movement, which becomes apparent when frames are composited into a single image and displayed sequentially over defined time intervals. In the case of frames demonstrating the direction of stock prices, the content change only involves two observations. With each subsequent frame, a new observation appears on the right side of the chart, and the oldest observation disappears. In this manner, consecutive frames demonstrate the dynamics of market price changes.

Figure 3 presents the base chart used to create a video for a single observation. We then divide this chart into frames, each being an image of 64x64 pixels in size, which is the standard dimension in video analysis algorithms. The figure demonstrates how the base chart is divided into frames, where the first few frames form the context for movement creation, and the subsequent frames become the subject of the forecast.

Three elements of the base chart’s construction become essential in using it to create a video for forecasting future stock prices. Firstly, the chart must have an appropriate width. Our single frame with a width of 64 pixels must demonstrate data for specific days, where the number of pixels for each day must be equal. We dedicate four pixels for a single daily observation. This size ensures a smooth line formation connecting individual observations for closing prices and moving averages. The lines would be very jagged with two pixels; three pixels are indivisible by 64, and a larger pixel count than four reduces the range of information on a single frame without providing noticeable benefits in chart smoothness. In

this case, a chart with a width of 64 pixels accommodates 16 observations.

When each observation is conditioned on the  $n$  preceding ones, the frames must differ by one observation. Hence, in the context of the base chart, expanding the number of displayed observations from 16 to 17 means expanding the chart from 64 to 68 pixels. However, Jiang et al. (2023) demonstrates that 20-day market data predicts future stock returns. To extend the range of input data for the model and to build a sufficient number of input frames with movement context, we use the first five video frames as input data for the model (observed period). In this approach, the first frame provides information within the scope of the first 16 observations (16 observations  $\times$  four pixels = 64 pixels). The subsequent four frames extend the number of observations to 20 and increase the base chart width to 80 pixels (16 observations  $\times$  4 pixels + four observations  $\times$  four pixels = 80 pixels).

When modeling financial data, each observation is conditioned on the preceding ones, meaning each frame in our representation must differ by one observation. In our base chart, expanding the number of displayed observations from 16 to 17 corresponds to expanding the chart from 64 to 68 pixels, as each observation is represented by four pixels.

However, Jiang et al. (2023) demonstrate that a 20-day market data window predicts future stock returns. We construct our input frames with a movement context in mind to align with this finding and extend our model's input data range.

Our approach uses the first five video frames as input data for the model during the observed period. The first frame provides information within the scope of the first 16 observations, translating to 64 pixels (16 observations multiplied by four pixels each).

The subsequent four frames do not add four complete sets of 16 observations; instead, they add one per frame, extending the total number of observations to 20. This increases the base chart width to 80 pixels, calculated as the original 16 observations multiplied by four pixels each, plus the additional four observations multiplied by four pixels each (16 observations  $\times$  4 pixels + 4 observations  $\times$  4 pixels = 80 pixels).

This methodology allows us to capture the temporal dynamics of the market, representing



the data in a way that reflects both the sequential nature of financial observations and the insights from existing research on market prediction

The design of our model includes a sequence of frames, where each frame represents a specific set of observations (e.g., price observations). The first frame encapsulates the initial 16 observations, represented by 64 pixels. Four subsequent frames add one observation, extending the total to 80 pixels. These frames correspond to observed data. Additional predictive frames forecast future observations, each requiring four pixels on the base chart. The model forecasts ten frames, expanding the base chart to a total width of 120 pixels. This structure allows for both the representation of observed data and sequential forecasting.

The second critical aspect of creating the base chart is the process of input data scaling. First, to eliminate the impact of price jumps associated with stock operations such as splits, we recalculate all chart elements based on the daily rate of returns, which are appropriately corrected by the CRSP (Jiang et al., 2023). Second, how the base chart elements are scaled significantly influences the potential look-ahead bias in the forecasting process.

Our model implements a chart scaling method that considers price and volume data based solely on observations from a specific period. This scaling method involves mapping the maximum and minimum prices and the top-level volume to specific pixel levels on the chart.

For illustration, let us assume that the scaling method sets the minimum price at a pixel level of 42 and the maximum at a pixel level of six.<sup>3</sup> The algorithm can learn from this pattern if the maximum price during the observed period only reaches a pixel level of 12 instead of six. Since the chart must touch the 42 and six-pixel points in each observation, the algorithm can infer that there should be a price increase to the six-pixel level in the forecast period. Figure 4 in the document illustrates this scaling method, showing how the data is scaled on the base graph.<sup>4</sup>

---

<sup>3</sup>In this context, lower pixel levels correspond to higher prices, and higher pixel levels correspond to lower prices. This mapping allows the algorithm to represent price movements within a defined pixel range, facilitating the learning and prediction.

<sup>4</sup>In our model, we represent financial data as a sequence of frames, with each observation mapped to a

The top-right chart is the pure input used to create frames, with dotted lines on the other three graphs marking the extreme values for prices (upper part of the chart) or volume (bottom part).

The potential issue is if we incorporate data from the forecast segment of the chart for scaling purposes, the algorithm could swiftly identify specific patterns. For instance, if the price maximum were to be within the forecast period instead of the observed period, the chart in the observed period would not reach the value typically necessary to achieve the maximum. Such a phenomenon would indicate to the algorithm that the price in the forecast period should attain the maximum value, thereby leading to the look-ahead bias.

Our model scales prices and volumes based on the extremes observed in the input period. This scaling method has an important implication: it can lead to situations where prices or volumes in the forecast period exceed the acceptable range of the chart.

To illustrate, consider the chart area for prices, represented between the first and 48th pixels. Within this range, the extremes for prices in the observed period are set at the 6th and 42nd pixels.<sup>56</sup> This means that the price can rise or fall by six pixels relative to the extreme in the input period before it reaches its maximum or minimum permissible level on the chart.

---

specific pixel level on a chart. The relationship between pixel levels and price levels is an arbitrary choice that serves our analytical needs, and it is not related to the conventional understanding of pixel resolution in digital images.

<sup>5</sup>We choose to represent the highest and lowest stock prices using the 6th and 42nd-pixel levels, respectively. This choice is based on carefully analyzing the observed price range in our dataset, where we map the historical extremes to these specific pixel values. By doing so, we ensure a standardized representation that accommodates the inherent variability of stock prices while maintaining a consistent scale across different stocks and periods. The choice of these particular pixel levels is not arbitrary but reflects our data's underlying distribution of prices. It allows us to translate pixel levels back into real-world price levels using the same scaling factors. This approach supports our analysis by providing a controlled yet flexible way to represent price movements, and it can be adapted to different datasets by recalibrating the scaling factors based on the observed price range.

<sup>6</sup>First, we can identify the minimum and maximum prices in the dataset to determine the range of prices. For example, let's say the minimum price is \$10, and the maximum price is \$100. Next, we determine the range of pixels. In our case, the 6th pixel represents the maximum price, and the 42nd pixel represents the minimum price. Third, we can calculate the scaling factor by dividing the price range by the pixels. In this example, the scaling factor would be  $(\$100 - \$10)/(6 - 42) = \$2.27$  per pixel. Lastly, we can convert pixel levels to prices by multiplying the pixel levels by the scaling factor and adding the minimum price. In this example, the 6th pixel would correspond to \$100, and the 42nd pixel would correspond to \$10.

However, we have implemented a safeguard to handle situations where the data exceeds this range. If a price or volume does exceed the acceptable range, we represent it by drawing a single pixel at the appropriate extreme on the chart. This approach ensures that the data remains within the chart’s defined bounds while still allowing some room for additional changes.

Figure 4, specifically the bottom-right panel, illustrates this situation. It shows how the scaling process accommodates extremes in the data, ensuring that the representation remains consistent and meaningful, even when unexpected fluctuations occur.

We create a flexible yet controlled data representation by scaling prices and volumes according to the observed extremes and implementing this safeguard. This approach supports our analysis while accommodating financial markets’ dynamic and sometimes unpredictable nature.

In summary, creating an image as a carrier of information about market states is an exact task where individual elements can significantly impact how the machine learning algorithm learns the dynamics of image changes. In the next section, we demonstrate the requirements behind the machine learning algorithm capable of understanding the market dynamics visualized as a video.

## 4 Model Selection

This section focuses on the Variational Recurrent Neural Networks (VRNN) model we employ for stock price forecasting. This model is pivotal in our research and serves several simultaneous functions we will elaborate on. This discourse aims to delineate the elements constituting the VRNN model and elucidate why a cohesive understanding of this model is imperative for accomplishing our research task.

Our model needs to fulfill several critical functions concurrently. Firstly, it must analyze data in the context of time series. Secondly, it must analyze the image and correctly

identify correlations among its elements. Thirdly, it must be capable of capturing highly uncertain correlations between the stock price at time  $t$  and market data from the preceding  $n$  observation days.

A vital aspect of our model is its capacity to forecast stock price levels rather than returns. Stock prices exhibit high autocorrelation, a highly desired phenomenon when forecasting subsequent video frames. Consequently, our model deviates from traditional financial models centered around forecasting returns and directly forecasts stock price levels.

Our model incorporates several advanced concepts known in artificial intelligence research to capture the high levels of uncertainty associated with the factors influencing stock price fluctuations. This section succinctly delineates the main tasks and capabilities of each applied algorithm.

At the outset of this section, a crucial point worth mentioning is that we delve into the task of video prediction, a specific manifestation of self-supervision where generative models learn to predict future frames in a video (Devlin, Chang, Lee, & Toutanova, 2018; Gidaris, Singh, & Komodakis, 2018). By undertaking this approach, we aim to establish a firm ground in the predictive modeling landscape.

## 4.1 Convolutional Neural Network

Convolutional Neural Networks (CNN) form our model’s backbone of image analysis, providing an effective means to identify dependencies among individual pixels on a chart. CNNs leverage a mathematical operation known as convolution to scan and process input data, allowing the model to identify and extract significant features from an image.

The fundamental idea behind CNNs involves using multiple layers of convolution and applying a set of learnable filters to the raw pixel data of an image. The convolution operation for a single 2D filter  $F$  of size  $a \times a$  applied to a part of the image  $I$  is defined as:

$$C_{ij} = \sum_{m=0}^{a-1} \sum_{n=0}^{a-1} I_{i+m,j+n} F_{m,n} \quad (1)$$

where  $C_{i,j}$  is the convolved feature (or feature map),  $I_{i+m,j+n}$  represents a portion of the image  $I$ , with the same size as the filter, that pixels' are located at  $i + m$  and  $j + n$ . Finally,  $F_{m,n}$  represents the elements of the filter  $F$  with  $m$  and  $n$  indicating the location of the elements within the filter. This process is repeated across all the image regions, effectively sliding the filter across the image and enabling the network to learn spatial hierarchies or patterns.

## 4.2 Recurrent Neural Networks

Stock price forecasting at time  $t$  based on market data from the previous  $n$  observations inherently entails time series analysis. Predicting sequences is a natural task for Recurrent Neural Networks (RNNs), a class of artificial neural networks designed to recognize patterns in data sequences.

RNNs can uniquely retain information from prior inputs in their hidden states, thereby modeling temporal dependencies. A basic form of an RNN can be represented as:

$$h_t = \sigma(W_{hh}h_{t-1} + W_{xh}x_t + b_h) \quad (2)$$

where  $h_t$  is the hidden state at time  $t$ ,  $x_t$  is the input at time  $t$ ,  $W_{xh}$ , and  $W_{hh}$  are weights,  $b_h$  is a bias, and  $\sigma$  is an activation function.

While models based on the combination of CNNs with a recurrent model, such as the Convolutional LSTM Network (Shi et al., 2015), are applicable for analyzing sequences of image frames, traditional RNNs fall short when accounting for forecast uncertainty due to their deterministic nature. Their only source of variability resides in the conditional output probability model, which is insufficient for capturing the randomness intrinsic to the data (Babaeizadeh, Finn, Erhan, Campbell, & Levine, 2017).

As demonstrated in Figure 5, typical probabilistic models, after applying the uncertainty, generate an average or 'shadow' of various potential scenarios when forecasting movements for

phenomena laden with high uncertainty. While indicating the most probable trajectory, these predictions are imprecise and thus inadequate for forecasting stock prices. This shortcoming necessitates the deployment of algorithms capable of predicting phenomena with high levels of uncertainty. The following sections discuss the implementation of such models, focusing on integrating Variational Autoencoders into RNN structures.

### 4.3 Variational Autoencoders

To enhance the efficacy of image series analysis, employing data compression of the images using autoencoders is practical. An autoencoder is a neural network architecture that consists of two main components: an encoder and a decoder. The encoder compresses high-dimensional image data into a compact space known as a bottleneck, and the decoder reconstructs the original data from this compressed representation (refer to Figure 6).

The compression is achieved by minimizing the reconstruction loss, which is the difference between the original input image and the output image generated by the decoder. A simple autoencoder utilizes fully connected layers of a neural network, but autoencoder layers can also encompass Convolutional Neural Network (CNN) cells, facilitating the compression of image or sound data.

However, traditional autoencoders map input data to a single vector, rendering them deterministic. This can be a limitation when modeling data with inherent variability. Non-deterministic models that map data onto a distribution are employed to address this. These models, known as Variational Autoencoders (VAEs), utilize two vectors—one for the mean and another for the standard deviation of the feature distribution (Kingma & Welling, 2013; Rezende, Mohamed, & Wierstra, 2014).

VAEs are a potent example of deep generational probabilistic graphical models adept at capturing input data variability and generating a distribution that summarizes this variability (refer to Figure 7). They offer a harmonious blend of flexible non-linear mapping between latent random states, observed outputs, and effective approximate inference. This

combination enables VAEs to model complex multimodal distributions, which are beneficial when the underlying true data distribution comprises multimodal conditional distributions.

The underlying principle of a VAE is rooted in Bayesian inference and can be expressed as follows:

$$q_\phi(z | x) = \mathcal{N}(z | \mu_\phi(x), \sigma_\phi^2(x)I) \quad (3)$$

where  $q_\phi(z | x)$  is the approximate posterior (encoder),  $\phi$  are the parameters of the encoder,  $z$  is the latent variable, and  $x$  is the observed data. The parameters  $\mu_\phi(x)$  and  $\sigma_\phi^2(x)$  of the Gaussian distribution are outputs of the encoder. The variational part of the VAE concerns minimizing the divergence between the true and approximate posterior.

Thanks to these modifications, VAEs can non-deterministically compress data and estimate various future states for each sample of their latent variables. The next section will leverage VAEs' properties and discuss their incorporation into the architecture of the Variational Recurrent Neural Network (VRNN).

## 4.4 Variational Recurrent Neural Network

The architecture of the Variational Recurrent Neural Network (VRNN) combines the temporal modeling capabilities of RNNs with the probabilistic latent variable modeling capabilities of VAEs, thereby enabling the creation of a powerful predictive model for complex and uncertain processes (Chung et al., 2015). At its core, the VRNN model embeds a VAE in each of the recurrent cells of the RNN.

This design allows the VRNN to handle the high uncertainty inherent in video frame prediction tasks. The variational component of the VRNN enables the generation of multiple plausible trajectories for object movement depicted in video frames, as opposed to a single deterministic trajectory.

VRNN is formulated with an architecture that closely intertwines the hidden states of the RNN ( $h_t$ ) with the latent variables of the VAE ( $z_t$ ) as shown by the following equations:

The prior:

$$p_{\theta}(z_t | h_{t-1}) = \mathcal{N}\left(z_t | \mu_{\theta}^{(p)}(h_{t-1}), \sigma_{\theta}^{(p)}(h_{t-1})\right) \quad (4)$$

The approximate posterior:

$$q_{\phi}(z_t | x_t, h_{t-1}) = \mathcal{N}\left(z_t | \mu_{\phi}^{(q)}(x_t, h_{t-1}), \sigma_{\phi}^{(q)}(x_t, h_{t-1})\right) \quad (5)$$

The observation model:

$$p_{\theta}(x_t | h_t) = \mathcal{N}\left(x_t | \mu_{\theta}^{(x)}(h_t), \sigma_{\theta}^{(x)}(h_t)\right) \quad (6)$$

The hidden state update:

$$h_t = f_{\theta}(h_{t-1}, z_t, x_t) \quad (7)$$

In the equations above,  $x_t$  denotes the input at time  $t$ ,  $z_t$  is the latent variable, and  $h_t$  is the hidden state. The parameters  $\theta$  and  $\phi$  represent the network parameters for the generative and inference models, respectively. The function  $f_{\theta}$  corresponds to the deterministic transition function of the RNN, which is usually a non-linear function such as a Long Short-Term Memory (LSTM) (Hochreiter & Schmidhuber, 1997) or Gated Recurrent Unit (GRU) (Cho et al., 2014).

Figure 8 presents a single cell of the VRNN model encapsulated within a dark red rectangle. This VRNN cell operates on the principles of a recurrent network, transforming the prior hidden state  $h_{t-1}$  into the current hidden state  $h_t$ . This  $h_t$  can be used in the following cell, establishing a temporal link across cells.

Inside the VRNN cell is a VAE that operates on the combined data of the prior hidden state  $h_{t-1}$  and the new frame  $x_t$ . It compresses this high-dimensional information using an encoder and a decoder equipped with CNN layers, facilitating pattern recognition in the input images.

In the VAE, the data is condensed into a latent vector  $z_t$  through a process based on two



key elements: the mean vector ( $\mu$ ) and the variance vector ( $\sigma$ ). This process can be seen in the Equation 5, where the input data  $x_t$  and the prior hidden state  $h_{t-1}$  are used to estimate the true distribution of the latent variable  $z_t$ .

The decoder part of the VAE relates to the Equation 4 and Equation 6, generating new frame data  $x_t$  from the hidden state  $h_t$ , and computing the distribution of the actual data. The deviation between this generated data and the actual data is termed the reconstruction error, which is minimized during training.

Finally, the VRNN cell uses a recursive function that integrates the information from the prior hidden state  $h_{t-1}$ , the current latent state  $z_t$ , and the new frame  $x_t$ . This process is represented by the Equation 7, which updates the hidden state  $h_t$  based on the previous hidden state, the current latent state, and the new input frame.

In conclusion, the diagram exhibits how the VRNN model leverages the strengths of RNNs, VAEs, and CNNs to handle complex, sequential data efficiently. It illustrates how each component - prior, approximate posterior, observation model, and hidden state update - contributes to the overall functioning of the model.

In conclusion, we demonstrate the connection between the RNN and VAE in the VRNN architecture, presenting a comprehensive understanding of how the VAE's non-deterministic nature is integrated into the RNN, thereby enhancing its capacity to handle high-uncertainty scenarios. The next section demonstrates the application of VRNN to finance.

## 5 Generating Future US Stock Prices as Video

In this chapter, we delve into our methodology, starting with a description of the data used in the study. Then, we explain the procedure for training the VRNN model to generate future frames. Further, we clarify how to read and interpret the data on the generated video frames. Finally, we present our results, beginning with the probability of determining the right direction of price changes, to showcase our model's economic applications in portfolio

construction.

## 5.1 Data

In our research, we utilize daily data from the Center for Research in Security Prices (CRSP) for constituents of the S&P500 index. Historical compositions of companies included in the index are acquired from Refinitiv. Our research sample pertains to the period from 1993 to 2021. Market data concerning the highest and lowest prices are available in CRSP since June 1992.

We focus on S&P500 index companies for several crucial reasons. First, our research involves forecasting daily stock price changes in the short term. Utilizing short-term forecasts to construct an investment portfolio necessitates frequent rebalancing and concurrent sufficient liquidity of analyzed companies. Concentrating on the largest U.S. companies in the S&P 500 ensures high liquidity and low transaction costs. This makes the results of our research applicable to investors with high assets. See Table 1 for the number of firms in our sample each year.

Second, a well-documented phenomenon is a decidedly lower predictability of the largest companies' stock prices.<sup>7</sup> Hence, by concentrating on the largest stocks, we demonstrate that our strategy achieves solid results amongst companies for which predicting the direction of price changes is most challenging.

Finally, the machine learning task of the next frame forecasting requires significant computational resources. A smaller number of companies in the analysis considerably accelerates calculations, making our study feasible even with commonly available computing equipment.

---

<sup>7</sup>Jiang et al. (2023) in their research use all companies listed on NYSE, AMEX, and NASDAQ. They show that the out-of-sample Sharpe ratio of strategies based on H-L decile spread portfolios sorted by image-based return is highest with a five-day rebalancing. Results for 20-day and 60-day rebalancing are significantly lower, and a Sharpe ratio above one is achievable only for equally weighted strategies. Value-weighted strategies reach a Sharpe ratio above one only with a weekly (five-day) rebalancing.

## 5.2 Training VRNN

Our task is to forecast the trajectory of market data changes for the next ten trading days using a method that involves both motion context and video frames. As mentioned in Section 3, we utilize five ‘context frames,’ which define the input data and signal the direction of object movement found on individual frames. These context frames encapsulate information from 20 trading days of historical market data, approximating one month (from  $t-19$  to  $t$ ), and predict 10 trading days of future market data that approximate two weeks (from  $t+1$  to  $t+10$ ). These changes encompass closing prices, maximum and minimum prices, the direction of a 20-day moving average, and volumes. By utilizing data other than closing prices, we aim to enhance the forecast capabilities related to future changes in the closing price.

To train the model, we generate 15 frames, comprising five context frames and ten forecast frames. This allows the model to learn the relationships between the context and forecast frames independently.

Our model’s design involves a base chart with a 64x120 pixel resolution, representing different dimensions or features of the market data, such as price and volume. We divide this chart into 15 parts, corresponding to five context frames (capturing 20 trading days of historical data) and ten forecast frames (predicting the next 10 trading days). The choice of 15 parts and the specific resolution aligns with our model’s architecture and the nature of the data.

We employ a sliding window method with a 64x64 resolution, moving the window by four pixels at a time across the base chart. This technique allows us to analyze sequential segments of the data, capturing temporal patterns and relationships.

Each observation in our model corresponds to the last trading day of a calendar week (day  $t$ ). While our data includes daily closing prices, we may have chosen this weekly reference point to align with other data sources, reduce noise, or capture specific market patterns relevant to our study.

Generative models, such as VRNNs, utilize specific measures to determine the degree of fit

between the generated image and the actual one. One such measure is the ‘loss,’ often called the reconstruction loss (`loss_rec`). This loss quantifies the discrepancy between the actual data and the reconstructed data generated by the model. The smaller the reconstruction loss, the more closely the generated data matches the actual data, indicating a better-performing model.

The second measure, ‘prior loss’ (`loss_prior`), deals with regularizing the latent variables in the VRNN. In simple terms, it ensures that the distribution of the latent variables follows a specific pattern, often a standard Gaussian distribution. By minimizing the prior loss, we encourage the latent variables to conform to this pattern, which can improve the model’s generative abilities.

Finally, the total ‘loss’ of the VRNN model is usually a combination of these two components: the reconstruction and prior losses. By minimizing these two components jointly, we aim to train a model that can effectively generate data similar to the training set while maintaining a regular structure in the latent space. Therefore, this loss function plays a crucial role in training our VRNN model and, subsequently, the quality of the predictions it generates.

Our study divides the data into a training period (1992-2000) and a testing period (2001-2021). We train the model once on the training data, setting aside several hundred of the last observations from the training set as a validation sample to measure the model’s training level. We determine the number of epochs necessary to train the model based on the total ‘loss’ in the validation sample and the early stopping approach.

All of our calculations are conducted using Python. We use the PyTorch package and perform demanding computations at the Foundry and Hellbender high-power computing environments at the University of Missouri.

### 5.3 Reading the Market Data from Video Frames

The output of our model consists of predicted frames. Accurately reading the data from these frames is crucial to conducting accuracy tests and applying these forecasts to portfolio construction. In this process, we examine each generated frame and read pixels from the relevant columns of the images, which correspond to the stock prices. We only search for white pixels, as closing prices are denoted in white. For instance, on the first generated frames, the first column of pixels on the right contains information about the forecasted closing price on the day  $t+1$ .

Subsequently, on the second of the generated frames, the fifth column of pixels from the right contains data for the same observation as the previous frame from day  $t+1$  but also includes an additional forecast in the first column from the right with the closing price from day  $t+2$ . Proceeding this manner, we arrive at the tenth generated frame, which contains forecasted prices for days  $t+1$  to  $t+10$ . We average all readings for the same days to eliminate potential noise or vagueness in the forecasts. The information read on the pixel's position forecasting the price on the day  $t+n$  can be compared with the reading of information about the pixel on the day  $t$ . This comparison provides the simplest yet effective way to verify whether the model has predicted a price increase, stability, or decrease for a specified number of days ahead. However, not only can the direction of changes be significant, but so can its scale. Therefore, forecasts differing by a larger (or smaller) number of pixels can be more (or less) important.

Finally, the number of days  $n$  utilized to forecast weekly price changes is also important. The maximum number of session days in a single week is five. Nevertheless, some weeks have fewer days. For this purpose, for each day  $t$ , representing the last session date in a given calendar week, we count the number of session days in the following calendar week. This calculation determines the number of session days in the next week. It serves as a reference point for choosing the appropriate length of the forecast from the data generated by the VRNN.

## 5.4 Accuracy of Forecasted Price Direction

Table 2 offers an intricate evaluation of the predictive power of our model over a spectrum of forecast durations. ‘Correct’ represents instances where the model’s forecasts accurately mirrored the observed market trajectory. For instance, the accuracy metric for a one-day-ahead forecast is pegged at 58%, showcasing a noteworthy precision level for near-term projections. Conversely, ‘Incorrect’ embodies situations where the model’s estimations diverged from actual outcomes. The consistency of the incorrect rates across different forecast horizons is evident, suggesting a stable predictive behavior of the model. Lastly, ‘Unclear’ alludes to cases where the model’s forecasts were neither distinctly correct nor incorrect, often due to ambiguities or inconclusiveness in the data visualization. This could arise from challenges in discerning a definitive market pattern, potentially stemming from data noise, heightened volatility, or multifaceted market dynamics.

One remarkable observation from Table 2 is the fairly uniform distribution of correct and incorrect rates, irrespective of the prediction horizon. However, a nuanced takeaway is the increase in unclear predictions as the forecast horizon extends, signaling an avenue for enhancement. While our model exhibits commendable accuracy for shorter durations, the escalating ambiguity for protracted horizons necessitates further refinements in the model’s architecture, data preprocessing techniques, and feature engineering to bolster its generalizability.

The results in Table 2 reveal some key insights. The correct and incorrect rates are similar across the length of the predicted period in days. Our correction rate is comparable with that of Jiang et al. (2023).

This table has some limitations. We do not report whether there is an asymmetric effect between negative and positive predictions. The correction presents the same direction of prediction for the actual and predicted value. Second, we do not consider the magnitude of the difference between actual and prediction. Although the model presents the correction that is greater than the incorrect one, the margin is narrow, between 12

## 5.5 Portfolio Performance

We analyze value-weighted and equal-weighted portfolios across five quintiles and find that returns and Sharpe ratios increased with each quintile. Our VRM strategy’s long-short portfolios produce the highest performance. See Table 3.

We also compare our results with non-machine learning strategies, including momentum (MOM), short-term reversal (ST\_REV), and long-term reversal (LT\_REV). Our equal-weighted and value-weighted portfolios generate higher Sharpe and Calmar ratios than these strategies. Specifically, VRM achieved Sharpe ratios of 2.47 and 2.94 for value-weighted and equal-weighted portfolios, respectively, while MOM achieves 0.05 and 0.01, ST\_REV achieves 0.24 and 0.51, and LT\_REV achieves 0.05 and 0.30.

As a benchmark, the CNN strategy of Jiang et al. (2023) generates Sharpe ratio of 0.96 and 0.78 for their value-weighted and equal-weighted portfolios, respectively, for the 500 largest stocks in their sample, which are comparable with us. Our Sharpe ratio is more than two times higher than that from their paper. Our methodology is composed of multiple steps and thus computing intensive. Table 4 shows our performance across transaction costs from one to ten basis points. The Sharpe ratio for value- and equal-weighted portfolio is still 1.26 to 2.49 (1.61 to 2.95) for transaction cost of 10 basis points to zero.

We assess our performance based on risk-adjusted returns and analyze the returns of our long-short portfolios sorted by predicted change in pixels in Table 5. Every week, we buy stocks in the top quintile of predicted pixel change and sell those in the bottom. Our estimation of risk-adjusted returns or alpha considers factors such as CAPM, FF3, FF5, FF6, Q4, DHS, short-term, and long-term reversal. Surprisingly, our alpha is highly significant, ranging from 0.0058 to 0.0059 with a t-stat of about 13 for equal-weighted and 0.0053 to 0.0058 for value-weighted portfolios with an average of 12. Our long-short strategy that sorts by predicted pixel change may provide a strong signal not captured by traditional factor models like CAPM, FF3, FF5, FF6, and DHS. This indicates that our alpha is significant and robust to different model specifications.

## 6 Mechanisms

We delve into the mechanics behind our strategy. To achieve this, we conduct the Fama-MacBeth cross-sectional regressions of the predicted change in pixels generated by our strategy on the firm-level trend strategies and characteristics presented in Table 6. In specification (1), we observe that our predicted change in pixels is negatively influenced by moving average returns over five, twenty, and sixty days. Specification (2) includes firm characteristics that are known to predict stock returns and trading, such as beta, bid-ask spread, trading volume, size, price delay, return volatility, and number of zero trades, as well as momentum returns from 1, 6, 12, and 36 months. These variables have been computed from the code provided by Green, Hand, and Zhang (2017), and are utilized by many studies, including Gu et al. (2020). The last specification pools all variables from specifications (1) and (2). We find that the moving average for 60 days survives, but the significance is weak at the 10% level. Size is also negative but weakly significant. The larger the size of the firm, the lower the change in pixels. Momentum one month and bid-ask spread are negative and highly significant at the 1% level. The higher the momentum and the larger the bid-ask spread, the lower the change in pixels. Illiquidity has been found to decrease a change in price movement. The CAPM beta is positive but weakly significant.

Moving forward, we explore whether the actual weekly change is in line with our forecasted change in pixel. Table 8 presents the Fama-MacBeth cross-sectional regression where we regress weekly returns on forecasted change in pixels and other characteristics that we have included in the previous table. Specification (1) shows that predicted change in pixels is positively correlated with weekly returns, but the correlation is not significant. Specification (2) includes all variables to alleviate omitted variable bias, in addition to pixel change predicting weekly returns. Pixel change becomes strongly significant at the 1% level. We rely on our conclusion based on this specification, as it includes important characteristics that are shown to predict firm returns. Overall, the result seems to support our forecasted change in pixel or price predicts stock returns.



## 7 Who Apply the VRNN strategy?

Our analysis delves into the adoption of the Variational Recurrent Neural Network (VRNN) strategy across different types of traders. To discern retail trading activity, we employ the methodology outlined by Boehmer, Jones, Zhang, and Zhang, 2021, calculating retail volume both in shares and U.S. dollars, normalized by the number of shares outstanding and market capitalization, respectively. Institutional trading data is derived from Thomson Reuters 13F filings, measuring changes in institutional holdings relative to stock market capitalization. In our empirical tests, detailed in Table 8, we regress the VRNN strategy’s predicted weekly returns—specifically, those derived from the first specification in Table 7—against metrics of retail and institutional trading, along with moving average returns and additional firm characteristics. Institutional trading emerges as highly significant at the 1% level, affirming its substantial correlation with the VRNN strategy’s application. Interestingly, retail trading also shows significance, albeit to a lesser extent, suggesting that a subset of retail traders, potentially the more sophisticated ones, might be utilizing this strategy. This observation holds true when analyzing the data based on the percentage of retail volume relative to the number of shares outstanding. Consequently, our findings robustly indicate that institutional traders are implementing the VRNN strategy, with unexpected but notable adoption among retail traders as well.

## 8 Conclusion

In conclusion, this research presents a novel approach to the prediction of stock price movements by using advanced machine learning techniques, particularly Variational Recurrent Neural Networks (VRNNs). By transforming daily price changes into visual representations and forecasting future trajectories, we’ve shown that our model delivers superior performance, especially for large, less predictable stocks. This approach holds significant implications for portfolio construction, particularly regarding liquidity and rebalancing strate-

gies.

Our research demonstrates the potential of machine learning in augmenting the understanding of financial market dynamics. However, it also acknowledges the limitations of this approach, including its computationally intensive nature and potential specificity to the market conditions of the training dataset.

Moving forward, it is clear that the fusion of machine learning and finance research can lead to significant advancements in understanding and predicting market trends. As technology evolves and computational resources become more accessible, adopting and refining such methods in finance are likely to continue and provide further insights into market dynamics. This study's results indicate promising future research directions, particularly in exploring the intricacies of market behavior using innovative computational methods.

We hope this study sparks further interest and research in this field, enabling more sophisticated models that can better capture the intricacies of financial markets and provide investors with superior tools for navigating the complexities of the market.

## Statement that describes main results and identifies their relevance to the Q Group mission

Our study, "Animating Stock Markets," introduces a groundbreaking method for predicting stock prices by leveraging the power of Variational Recurrent Neural Networks (VRNNs). This novel approach transforms complex market data into dynamic, graph-based narratives that unfold like a movie. By analyzing S&P 500 constituents from 1993 to 2021, our model achieves Sharpe ratios of 2.94 for equally weighted and 2.47 for value-weighted portfolios, with an alpha of 55 weekly basis points adjusted for established risk factors.

The core of our research lies in utilizing historical stock prices, akin to video frames, to forecast future price trajectories more accurately. Traditional models often rely on returns due to the non-stationarity of stock prices. However, our approach directly analyzes prices, recognizing them as the primary carriers of market information. Prices embody the "memory of markets," encompassing the history of public and private events related to a company. This method allows us to capture significant turning points and trends, enhancing the predictability of stock price movements.

Inspired by generative algorithms used in short-term weather forecasting, our research applies these techniques to financial data. By treating stock price movements as sequential video frames, our VRNN model effectively captures the temporal and spatial dependencies inherent in market data. This dynamic perspective allows for a more holistic understanding of market behavior, significantly improving prediction accuracy over traditional models.

Our results demonstrate that the VRNN model's ability to predict pixel changes robustly forecasts weekly returns, considering various price trend strategies and firm characteristics. The correlation of our predicted returns with institutional trading is substantial, highlighting the practical applicability of our approach.

In conclusion, our study advances financial forecasting by integrating advanced machine learning techniques with a cinematic approach to data analysis. This innovative methodology offers profound implications for trading strategies and risk management, providing a robust tool for investors and financial analysts.

## References

- Babaeizadeh, M., Finn, C., Erhan, D., Campbell, R., & Levine, S. (2017). Stochastic Variational Video Prediction. *6th International Conference on Learning Representations, ICLR 2018 - Conference Track Proceedings*. arXiv: [1710.11252](https://arxiv.org/abs/1710.11252)
- Bi, K., Xie, L., Zhang, H., Chen, X., Gu, X., & Tian, Q. (2023). Accurate medium-range global weather forecasting with 3d neural networks. *Nature*, 1–6.
- Boehmer, E., Jones, C. M., Zhang, X., & Zhang, X. (2021). Tracking retail investor activity. *The Journal of Finance*, *76*(5), 2249–2305.
- Chen, L., Pelger, M., & Zhu, J. (2023). Deep learning in asset pricing. *Management Science*.
- Cho, K., Van Merriënboer, B., Gulcehre, C., Bahdanau, D., Bougares, F., Schwenk, H., & Bengio, Y. (2014, June). Learning phrase representations using RNN encoder-decoder for statistical machine translation. In *Emnlp 2014 - 2014 conference on empirical methods in natural language processing, proceedings of the conference* (pp. 1724–1734). doi:[10.3115/v1/d14-1179](https://doi.org/10.3115/v1/d14-1179). arXiv: [1406.1078](https://arxiv.org/abs/1406.1078)
- Chung, J., Kastner, K., Dinh, L., Goel, K., Courville, A. C., & Bengio, Y. (2015). A Recurrent Latent Variable Model for Sequential Data. *Advances in Neural Information Processing Systems*, *28*
- Daniel, K., Hirshleifer, D., & Sun, L. (2020). Short-and long-horizon behavioral factors. *The review of financial studies*, *33*(4), 1673–1736.
- Devlin, J., Chang, M. W., Lee, K., & Toutanova, K. (2018). BERT: Pre-training of Deep Bidirectional Transformers for Language Understanding. *NAACL HLT 2019 - 2019 Conference of the North American Chapter of the Association for Computational Linguistics: Human Language Technologies - Proceedings of the Conference*, *1*, 4171–4186. arXiv: [1810.04805](https://arxiv.org/abs/1810.04805)
- Ebert, F., Finn, C., Lee, A. X., & Levine, S. (2017). Self-supervised visual planning with temporal skip connections. arXiv: [1710.05268](https://arxiv.org/abs/1710.05268) [[cs.R0](https://arxiv.org/abs/1710.05268)]
- Fama, E. F., & French, K. R. (2018). Choosing factors. *Journal of financial economics*, *128*(2), 234–252.
- Feng, G., He, J., & Polson, N. G. (2018). Deep learning for predicting asset returns. *arXiv preprint arXiv:1804.09314*.
- Frazzini, A., Israel, R., & Moskowitz, T. J. (2018). Trading costs. *Available at SSRN 3229719*.
- Gidaris, S., Singh, P., & Komodakis, N. (2018). Unsupervised Representation Learning by Predicting Image Rotations. *6th International Conference on Learning Representations, ICLR 2018 - Conference Track Proceedings*. arXiv: [1803.07728](https://arxiv.org/abs/1803.07728)
- Green, J., Hand, J. R., & Zhang, X. F. (2017). The characteristics that provide independent information about average us monthly stock returns. *The Review of Financial Studies*, *30*(12), 4389–4436.
- Gu, S., Kelly, B., & Xiu, D. (2020). Empirical asset pricing via machine learning. *The Review of Financial Studies*, *33*(5), 2223–2273.
- Hochreiter, S., & Schmidhuber, J. (1997). Long Short-Term Memory. *Neural Computation*, *9*(8), 1735–1780. doi:[10.1162/neco.1997.9.8.1735](https://doi.org/10.1162/neco.1997.9.8.1735)
- Hou, K., Mo, H., Xue, C., & Zhang, L. (2021). An augmented q-factor model with expected growth. *Review of Finance*, *25*(1), 1–41.

- Jiang, J., Kelly, B., & Xiu, D. (2023). (re-)imag(in)ing price trends. *The Journal of Finance*, 78(6), 3193–3249.
- Jiang, J., Kelly, B. T., & Xiu, D. (2020). (re-)imag(in)ing price trends. *Capital Markets: Asset Pricing & Valuation eJournal*.
- Ke, Z. T., Kelly, B. T., & Xiu, D. (2019). *Predicting returns with text data*. National Bureau of Economic Research.
- Kingma, D. P., & Welling, M. (2013). Auto-Encoding Variational Bayes. *2nd International Conference on Learning Representations, ICLR 2014 - Conference Track Proceedings*. arXiv: [1312.6114](https://arxiv.org/abs/1312.6114)
- Obaid, K., & Pukthuanthong, K. (2022). A picture is worth a thousand words: Measuring investor sentiment by combining machine learning and photos from news. *Journal of Financial Economics*, 144(1), 273–297.
- Rezende, D. J., Mohamed, S., & Wierstra, D. (2014). Stochastic Backpropagation and Approximate Inference in Deep Generative Models. *31st International Conference on Machine Learning, ICML 2014*, 4, 3057–3070. arXiv: [1401.4082](https://arxiv.org/abs/1401.4082)
- Shi, X., Chen, Z., Wang, H., Yeung, D.-Y., Wong, W.-K., Woo, W.-C., & Kong Observatory, H. (2015). Convolutional LSTM Network: A Machine Learning Approach for Precipitation Nowcasting. *Advances in Neural Information Processing Systems*, 28.

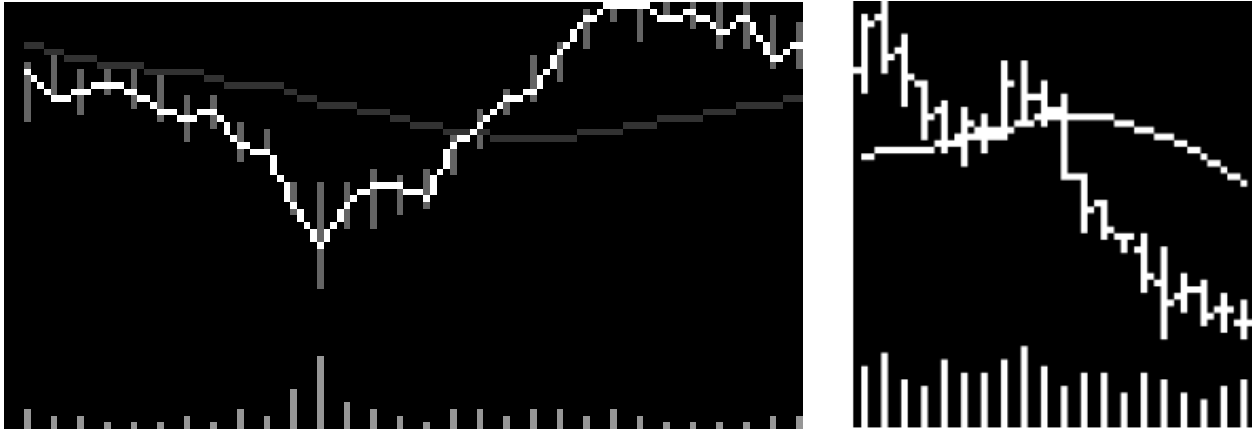


**Figure 1:** Graphs comparison

In this figure, we show a comparison between two graphs. The graph on the left is the base graph that we use to create frames for animations that, with 20 days historical daily observation predict up to 10 days of future market data. On the right, we show a graph prepared by Jiang, Kelly, and Xiu (2020) where 20 historical daily observations are used to predict the price direction in 5, 20, or 60 days.

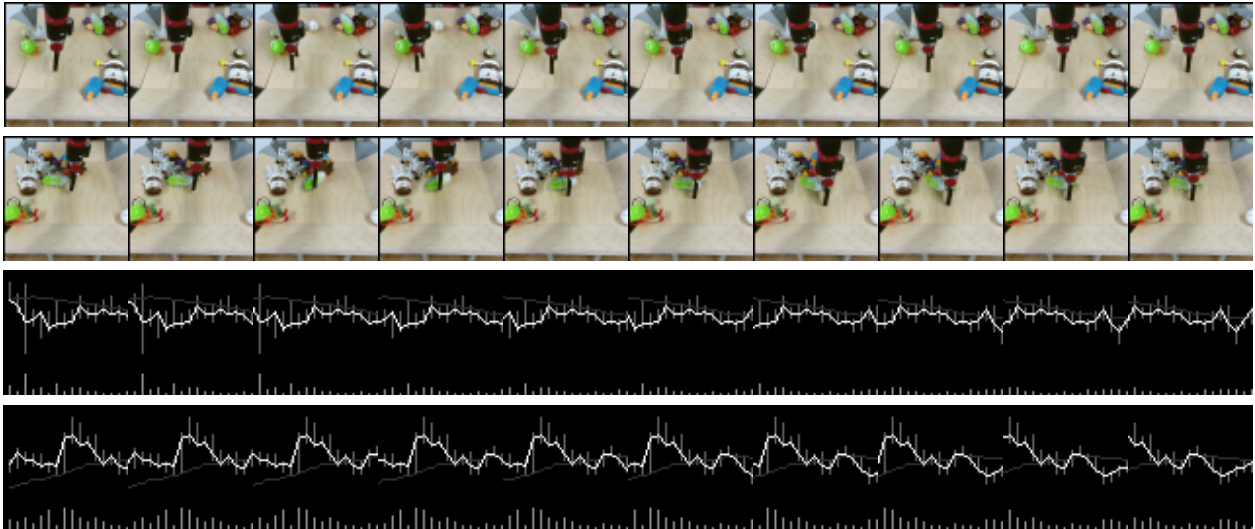


**Figure 2:** Sample video frames

This figure presents sample frames of four videos. Each video consists of ten frames. Two upper rows demonstrate frames from video database BAIR Robot Pushing frequently used by researchers to test algorithms dedicated to next frame forecasting task (Ebert, Finn, Lee, & Levine, 2017). Two bottom rows show frames from graphs created in this research.

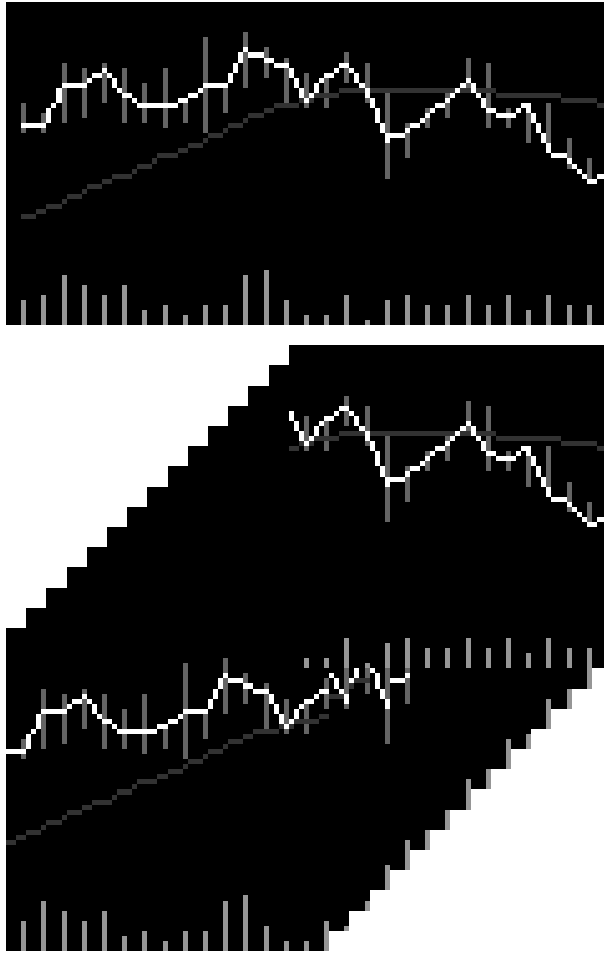


**Figure 3:** Frames of a Video from a Base Chart

This figure demonstrates the transformation of a base chart into frames. The base chart (at the top of the figure) has dimension 64x120 pixels. It is separated into 15 frames (at the bottom of the figure) with dimension 64x64 pixels. The first frame and the last are demonstrated in the front of others.

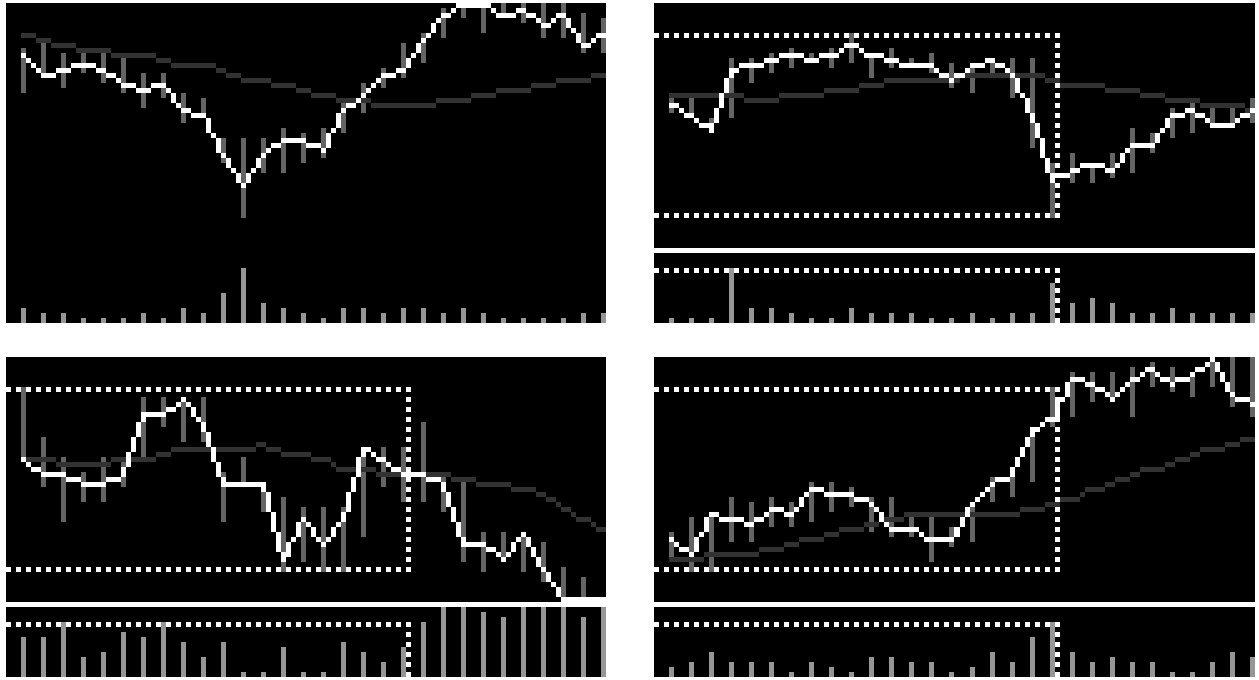


**Figure 4:** The data scaling procedure

This figure demonstrates how we scale the data on the base graph. We present four base graphs that are used to form video frames. The top-right chart is a pure input to create frames. On the other three graphs, we add, for information purposes, dotted lines that demonstrate the borders forming extreme values for prices (upper part of the chart) or volume (bottom part).

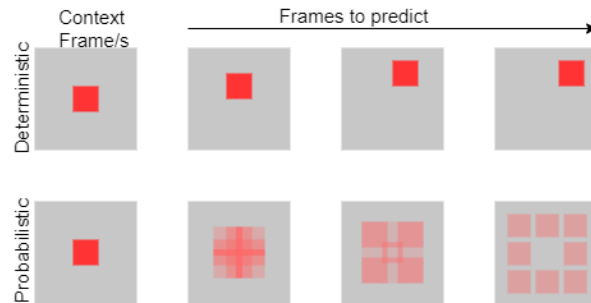


**Figure 5:** Generative Outcome of Deterministic vs. Probabilistic Model

The top part demonstrates frames of deterministic model where a box moves in a random direction. The bottom part, shows a probabilistic outcome. By introducing the uncertainty the generated objects are blurry and averaged. Figure inspired by Babaeizadeh, Finn, Erhan, Campbell, and Levine (2017).



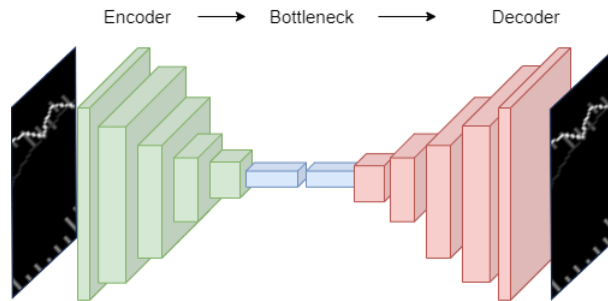


**Figure 6:** Autoencoder

In autoencoder the input data is compressed with encoder to bottleneck and then it is decompressed with decoder. In the training process the algorithm's task it to minimize the comparison error between the original input and the decoded output.

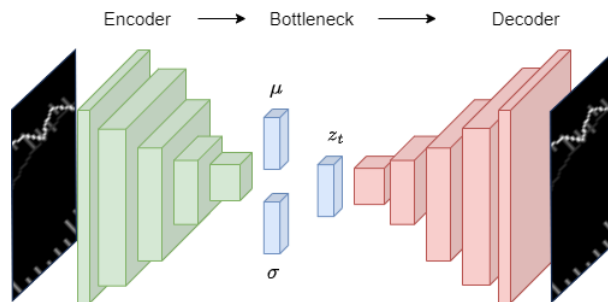


**Figure 7:** Variational Autoencoder (VAE)

Variational autoencoder is a type of autoencoder where encoder takes input and output two vectors, one with the means and the other with variance. Next, mean and variance vector are used to create a sampled vector. The decoder reconstruct input from the sampled vector.

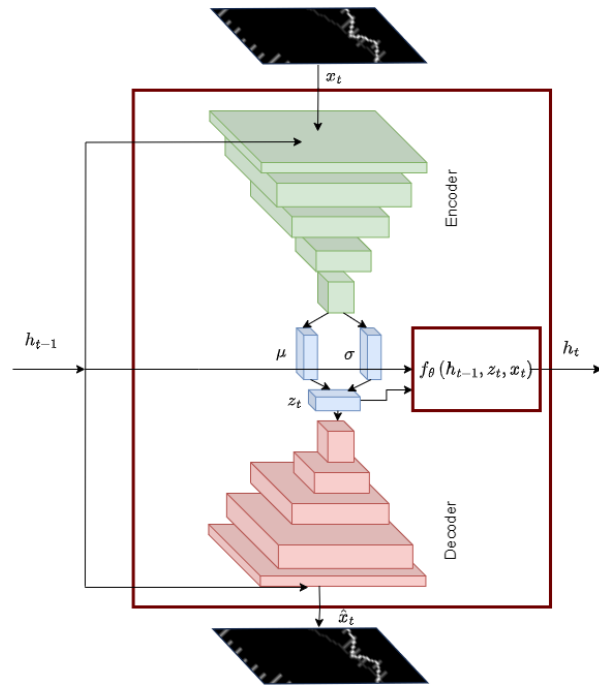


**Figure 8:** Variational Recurrent Neural Network (VRNN)

The figure illustrates a single Variational Recurrent Neural Network (VRNN) cell. In VRNN each cell contains a Variational Autoencoder (VAE) with Convolutional Neural Network (CNN) layers, which condenses high-dimensional data into a low-dimensional latent vector. The prior hidden state ( $h_{t-1}$ ), current latent state ( $z_t$ ), and new input frame ( $x_t$ ) are processed through a recursive function to yield the current hidden state ( $h_t$ ).

**Table 1:** Descriptive Statistics

The table presents an overview of the research sample (SAMPLE) vs. S&P500 Index (S&P500) in yearly periods. Stocks in the research sample demonstrate equal-weight average weekly returns (RetEw), value-weight average weekly returns (RetVw), total market capitalization in millions of dollars (Mcap), and number of stocks (No). The data for S&P Index covers market capitalization in millions of dollars (Mcap).

| year | Sample |       |        |     | S&P500 |
|------|--------|-------|--------|-----|--------|
|      | RetEw  | RetVw | Mcap   | No  | Mcap   |
| 2001 | 0.18   | 0.13  | 8,737  | 444 | 10,731 |
| 2002 | -0.32  | -0.28 | 7,459  | 438 | 9,143  |
| 2003 | 0.70   | 0.59  | 7,322  | 436 | 8,900  |
| 2004 | 0.35   | 0.29  | 8,551  | 439 | 10,522 |
| 2005 | 0.18   | 0.19  | 9,084  | 441 | 11,060 |
| 2006 | 0.31   | 0.38  | 9,747  | 449 | 11,849 |
| 2007 | 0.03   | 0.20  | 10,871 | 451 | 13,141 |
| 2008 | -0.81  | -0.50 | 8,924  | 457 | 10,666 |
| 2009 | 0.92   | 0.75  | 7,096  | 449 | 8,295  |
| 2010 | 0.43   | 0.38  | 8,578  | 442 | 10,288 |
| 2011 | 0.07   | 0.18  | 9,514  | 443 | 11,554 |
| 2012 | 0.28   | 0.32  | 10,248 | 438 | 12,445 |
| 2013 | 0.67   | 0.64  | 11,999 | 433 | 14,664 |
| 2014 | 0.31   | 0.37  | 14,033 | 430 | 17,197 |
| 2015 | -0.04  | 0.08  | 14,772 | 439 | 18,217 |
| 2016 | 0.31   | 0.32  | 14,699 | 437 | 18,197 |
| 2017 | 0.38   | 0.47  | 16,938 | 443 | 21,027 |
| 2018 | -0.19  | -0.05 | 18,699 | 438 | 23,293 |
| 2019 | 0.54   | 0.64  | 19,511 | 431 | 24,315 |
| 2020 | 0.43   | 0.61  | 21,820 | 440 | 26,622 |
| 2021 | 0.51   | 0.58  | 28,733 | 440 | 36,176 |

**Table 2:** Accuracy of Predicted Price Direction

This table reports the out-of-sample accuracy of price change direction depending on the length of the predicted period in days. We define the positive direction as not smaller than zero and the negative direction as less than zero. The correct predictions state that the model predicts positive (negative) price change when the price change is positive (negative) and incorrect demonstrate that the model predicts positive (negative) and it is negative (positive). The unclear observations denote graphs where the pixels displaying closing prices are unavailable. We calculate accuracy by dividing the number of correct (incorrect) observations by the total number of clear observations. The share of unclear observations is estimated as the number of unclear observations to the total number of samples.

|           | 1    | 2    | 3    | 4    | 5    | 6    | 7    | 8    | 9    | 10   |
|-----------|------|------|------|------|------|------|------|------|------|------|
| Correct   | 0.58 | 0.57 | 0.56 | 0.56 | 0.56 | 0.56 | 0.56 | 0.56 | 0.56 | 0.57 |
| Incorrect | 0.42 | 0.43 | 0.44 | 0.44 | 0.44 | 0.44 | 0.44 | 0.44 | 0.44 | 0.43 |
| Unclear   | 0.04 | 0.05 | 0.05 | 0.06 | 0.07 | 0.07 | 0.07 | 0.07 | 0.07 | 0.29 |

**Table 3: Portfolio Performance**

The table compares the performance of value-weight (Panel A) and equal-weight (Panel B) quintile portfolios sorted by the out-of-sample pixel change for the next week predicted by our VRNN model. Animated Stock Market portfolio (ASM) is sorted on out-of-sample predicted pixel change for the next week. Momentum (MOM), short-term reversal (ST\_REV), and LT\_REV portfolios are sorted on prior monthly returns 12-2, 1-0, and 60-13, respectively. Panels report annual return (Ret), annualized standard deviation (SD), maximum drawdown (MD), Sharpe ratio (SR), and Calmar Ratio (CR).

| <b>PANEL A: Value-Weight</b> |       |      |      |       |       |            |      |      |      |      |               |      |      |      |      |               |      |      |       |       |
|------------------------------|-------|------|------|-------|-------|------------|------|------|------|------|---------------|------|------|------|------|---------------|------|------|-------|-------|
| <b>ASM</b>                   |       |      |      |       |       | <b>MOM</b> |      |      |      |      | <b>ST_REV</b> |      |      |      |      | <b>LT_REV</b> |      |      |       |       |
|                              | Ret   | SD   | MD   | SR    | CR    | Ret        | SD   | MD   | SR   | CR   | Ret           | SD   | MD   | SR   | CR   | Ret           | SD   | MD   | SR    | CR    |
| Low                          | 0.03  | 0.17 | 0.74 | 0.15  | 0.04  | 0.10       | 0.31 | 0.79 | 0.31 | 0.12 | 0.07          | 0.18 | 0.62 | 0.40 | 0.12 | 0.10          | 0.22 | 0.53 | 0.44  | 0.19  |
| 2                            | 0.11  | 0.16 | 0.51 | 0.68  | 0.22  | 0.11       | 0.19 | 0.57 | 0.59 | 0.20 | 0.09          | 0.15 | 0.47 | 0.61 | 0.20 | 0.10          | 0.17 | 0.53 | 0.62  | 0.19  |
| 3                            | 0.16  | 0.16 | 0.39 | 1.00  | 0.42  | 0.11       | 0.15 | 0.47 | 0.74 | 0.24 | 0.10          | 0.15 | 0.45 | 0.70 | 0.23 | 0.09          | 0.15 | 0.48 | 0.64  | 0.20  |
| 4                            | 0.19  | 0.17 | 0.40 | 1.11  | 0.47  | 0.11       | 0.14 | 0.41 | 0.75 | 0.26 | 0.12          | 0.18 | 0.50 | 0.66 | 0.24 | 0.11          | 0.14 | 0.44 | 0.83  | 0.26  |
| High                         | 0.31  | 0.16 | 0.25 | 1.87  | 1.23  | 0.11       | 0.17 | 0.51 | 0.66 | 0.22 | 0.12          | 0.26 | 0.75 | 0.45 | 0.15 | 0.11          | 0.17 | 0.54 | 0.63  | 0.20  |
| H-L                          | 0.28  | 0.11 | 0.15 | 2.47  | 1.84  | 0.01       | 0.27 | 0.70 | 0.05 | 0.02 | 0.04          | 0.18 | 0.49 | 0.24 | 0.09 | 0.01          | 0.15 | 0.56 | 0.05  | 0.01  |
| <b>PANEL B: Equal-Weight</b> |       |      |      |       |       |            |      |      |      |      |               |      |      |      |      |               |      |      |       |       |
| Low                          | -0.00 | 0.19 | 0.80 | -0.02 | -0.01 | 0.15       | 0.30 | 0.69 | 0.50 | 0.22 | 0.10          | 0.21 | 0.62 | 0.47 | 0.16 | 0.17          | 0.26 | 0.64 | 0.66  | 0.27  |
| 2                            | 0.08  | 0.19 | 0.63 | 0.43  | 0.13  | 0.15       | 0.20 | 0.60 | 0.72 | 0.24 | 0.13          | 0.18 | 0.56 | 0.72 | 0.23 | 0.14          | 0.19 | 0.57 | 0.72  | 0.24  |
| 3                            | 0.13  | 0.19 | 0.60 | 0.66  | 0.21  | 0.14       | 0.17 | 0.52 | 0.83 | 0.28 | 0.14          | 0.18 | 0.57 | 0.75 | 0.24 | 0.14          | 0.17 | 0.51 | 0.80  | 0.27  |
| 4                            | 0.17  | 0.19 | 0.50 | 0.87  | 0.34  | 0.15       | 0.16 | 0.47 | 0.90 | 0.31 | 0.15          | 0.20 | 0.63 | 0.71 | 0.23 | 0.13          | 0.17 | 0.54 | 0.76  | 0.24  |
| High                         | 0.30  | 0.19 | 0.40 | 1.59  | 0.75  | 0.15       | 0.19 | 0.56 | 0.79 | 0.27 | 0.17          | 0.28 | 0.63 | 0.61 | 0.27 | 0.13          | 0.20 | 0.57 | 0.65  | 0.23  |
| H-L                          | 0.30  | 0.10 | 0.13 | 2.94  | 2.31  | 0.00       | 0.23 | 0.71 | 0.01 | 0.00 | 0.08          | 0.15 | 0.20 | 0.51 | 0.38 | -0.04         | 0.14 | 0.73 | -0.30 | -0.06 |

**Table 4:** VRNN Portfolios vs. Transactions Costs

The table presents the impact of transaction costs on the strategy performance and the average monthly turnover. Panel A shows the performance of value-weight portfolios and Panel B of the equal-weight. Panels report annual return (Ret), Sharpe ratio (SR), Calmar Ratio (CR), and average monthly turnover (Turnover).

| <b>PANEL A: Value-Weight</b> |       |       |       |       |       |       |       |       |       |       |       |
|------------------------------|-------|-------|-------|-------|-------|-------|-------|-------|-------|-------|-------|
|                              | 0.00% | 0.01% | 0.02% | 0.03% | 0.04% | 0.05% | 0.06% | 0.07% | 0.08% | 0.09% | 0.10% |
| Ret                          | 0.28  | 0.27  | 0.25  | 0.24  | 0.23  | 0.21  | 0.20  | 0.18  | 0.17  | 0.16  | 0.14  |
| SR                           | 2.49  | 2.36  | 2.24  | 2.12  | 1.99  | 1.87  | 1.75  | 1.63  | 1.50  | 1.38  | 1.26  |
| CR                           | 1.85  | 1.74  | 1.64  | 1.53  | 1.43  | 1.33  | 1.23  | 1.14  | 1.04  | 0.95  | 0.86  |
| Turnover                     | 1156% |       |       |       |       |       |       |       |       |       |       |
| <b>PANEL B: Equal-Weight</b> |       |       |       |       |       |       |       |       |       |       |       |
| Ret                          | 0.30  | 0.29  | 0.27  | 0.26  | 0.24  | 0.23  | 0.22  | 0.20  | 0.19  | 0.18  | 0.16  |
| SR                           | 2.95  | 2.82  | 2.68  | 2.55  | 2.42  | 2.28  | 2.15  | 2.01  | 1.88  | 1.75  | 1.61  |
| CR                           | 2.32  | 2.19  | 2.06  | 1.94  | 1.82  | 1.70  | 1.58  | 1.47  | 1.35  | 1.25  | 1.14  |
| Turnover                     | 1121% |       |       |       |       |       |       |       |       |       |       |

**Table 5:** Alphas from the VRNN-based strategy

This table presents alpha from regressing the equal-weighted and value-weighted returns of the long-short portfolios sorted by the out-of-sample predicted pixel change for the next week. The independent variables are the factors from CAPM, FF3, FF5, FF6, DHS, and all combined. \*\*\*, \*\*, and \* present one, five and ten percent significance, respectively.

| Model        | <b>Equal-Weight</b> |        | <b>Value-Weight</b> |        |
|--------------|---------------------|--------|---------------------|--------|
|              | Coefficient         | t-stat | Coefficient         | t-stat |
| CAPM         | 0.0058***           | 13.28  | 0.0054***           | 11.75  |
| FF3          | 0.0058***           | 13.26  | 0.0058***           | 13.26  |
| FF5          | 0.0058***           | 13.41  | 0.0056***           | 12.04  |
| FF6          | 0.0058***           | 13.45  | 0.0056***           | 12.10  |
| Q4           | 0.0059***           | 13.35  | 0.0055***           | 11.87  |
| DHS          | 0.0059***           | 13.58  | 0.0056***           | 12.20  |
| All+STR +LTR | 0.0059***           | 13.49  | 0.0053***           | 11.03  |

**Table 6:** VRNN on stock characteristics

This table presents the Fama-MacBeth cross-sectional regression. The dependent variable is predicted pixels change in a one-week horizon based on our VRNN model. The independent variables are lagged and collected from Gu, Kelly, and Xiu, 2020. `Mov_avg_Ndays` is the moving average of daily returns over N days. `Mov_avg_Ndays` are lagged by one week, the monthly variables such as momentum (`mom`) variables are lagged by one month, and other variables are lagged annually, consistent with the original paper. The standard errors are Newey-West adjusted. \*\*\*, \*\*, and \* present one, five, and ten percent significance, respectively.

|                            | (1)                     | (2)                     |
|----------------------------|-------------------------|-------------------------|
| <b>Dep. Variable:</b>      | Predicted Pixels Change | Predicted Pixels Change |
| <code>mov_av_est_5</code>  | -0.056**                | -0.016                  |
| <code>mov_av_est_20</code> | -0.058**                | -0.021*                 |
| <code>mov_av_est_60</code> | -0.051*                 | -0.011*                 |
| <code>mve</code>           |                         | -0.006*                 |
| <code>mom6m</code>         |                         | -0.002                  |
| <code>mom12m</code>        |                         | 0.005                   |
| <code>mom36m</code>        |                         | 0.008                   |
| <code>mom1m</code>         |                         | -0.009***               |
| <code>dolvol</code>        |                         | -0.017                  |
| <code>retvol</code>        |                         | -0.001**                |
| <code>baspread</code>      |                         | -0.001***               |
| <code>ill</code>           |                         | -0.000*                 |
| <code>zerotrade</code>     |                         | 0.000**                 |
| <code>BETA</code>          |                         | 0.005*                  |
| <code>pricedelay</code>    |                         | 0.001                   |
| <code>R2</code>            | 0.003                   | 0.013                   |

**Table 7:** Future returns on VRNN and stock characteristics

This table presents the Fama-MacBeth cross-sectional regression. The dependent variable is a weekly return. The independent variables are predicted pixels based on our VRNN model, `Mov_avg_Ndays`, and lagged characteristics collected from Gu, Kelly, and Xiu, 2020. `Mov_avg_Ndays` is the moving average of daily returns over N days. The `Mov_avg_Ndays` are lagged by one week, monthly variables such as momentum (`mom`) variables are lagged by one month, and other variables are lagged annually, consistent with the original paper. The standard errors are Newey-West adjusted. \*\*\*, \*\*, and \* present one, five, and ten percent significance, respectively.

|                            | (1)     | (2)     | (3)      |
|----------------------------|---------|---------|----------|
| <b>Dep. Variable</b>       | WeekRet | WeekRet | WeekRet  |
| <code>pred_week</code>     | 0.145   |         | 0.289*** |
| <code>mov_av_est_5</code>  |         | 0.026   | 0.005    |
| <code>mov_av_est_20</code> |         | 0.027   | 0.005    |
| <code>mov_av_est_60</code> |         | 0.031   | 0.003    |
| <code>mve</code>           |         |         | -0.001   |
| <code>mom6m</code>         |         |         | -0.003   |
| <code>mom12m</code>        |         |         | -0.006   |
| <code>mom36m</code>        |         |         | 0.001    |
| <code>mom1m</code>         |         |         | -0.000   |
| <code>dolvol</code>        |         |         | 0.000    |
| <code>retvol</code>        |         |         | 0.000    |
| <code>baspread</code>      |         |         | 0.000    |
| <code>ill</code>           |         |         | 0.000    |
| <code>zerotrade</code>     |         |         | -0.000   |
| <code>BETA</code>          |         |         | 0.002    |
| <code>pricedelay</code>    |         |         | -0.001   |
| <code>R2</code>            | 0.002   | 0.012   | 0.024    |

**Table 8:** Predicted returns from VRNN strategy and retail vs. institutional trading

This table presents the Fama-MacBeth regression. The dependent variable is the predicted weekly return from the VRNN strategy or the predicted returns in the specification (1) in Table 7. The independent variables are retail trading volume per stock market cap, institutional trading per market cap, Mov\_avg\_Ndays, and lagged characteristics collected from Gu, Kelly, and Xiu, 2020. Mov\_avg\_Ndays is the moving average of daily returns over N days. The Mov\_avg\_Ndays are lagged by one week, monthly variables such as momentum (mom) variables are lagged by one month, and other variables are lagged annually, consistent with the original paper. The standard errors are Newey-West adjusted. \*\*\*, \*\*, and \* present one, five, and ten percent significance, respectively.

| (3)                   |                         |
|-----------------------|-------------------------|
| Dep. Variable         | Predicted Weekly Return |
| Retail trading        | 0.171*                  |
| Institutional trading | 0.245***                |
| mov_av_est_5          | 0.016                   |
| mov_av_est_20         | 0.004                   |
| mov_av_est_60         | 0.002                   |
| mve                   | -0.013**                |
| mom6m                 | -0.004                  |
| mom12m                | -0.005                  |
| mom36m                | 0.003                   |
| mom1m                 | -0.000                  |
| dolvol                | 0.000                   |
| retvol                | 0.001                   |
| baspread              | 0.002                   |
| ill                   | 0.000                   |
| zerotrade             | -0.001                  |
| BETA                  | 0.001                   |
| pricedelay            | -0.001                  |
| R2                    | 0.027                   |